# Literature Review And Experiments On Waste Package Corrosion—Copper And Carbon Steel

*Prepared for*

**U.S. Nuclear Regulatory Commission**
**Contract NRC–HQ–12–R–02–0126**

*Prepared by*

**Xihua He[1]**
**Tae Ahn[2]**
**Jude McMurry[2]**

**[1]Center for Nuclear Waste Regulatory Analyses**
**San Antonio, Texas**

**[2]U.S. Nuclear Regulatory Commission**
**Washington DC**

**March 2015**

# CONTENTS

# FIGURES

# TABLES

# EXECUTIVE SUMMARY

Copper and carbon steel are being considered as candidate materials for waste packages in geologic disposal systems for high-level radioactive waste where the repository is located in the saturated zone below the water table.  The environment is expected to evolve from initially oxidizing, to anoxic, and eventually to reducing.  Within an anoxic environment, copper is reported to exhibit either a very low corrosion rate when exposed to groundwater or, theoretically, to experience no corrosion when it is in thermodynamic equilibrium with the groundwater.  Carbon steel is a corrosion-allowance material that is reported to have low corrosion rates (several micrometers per year) in simulated reducing groundwater, such that a carbon steel waste package could last for thousands of years.  Because of the importance of corrosion behavior of waste package materials to repository performance, it is considered as an important technical issue in high-level waste (HLW) disposal.  The U.S. Nuclear Regulatory Commission (NRC) directed the Center for Nuclear Waste Regulatory Analyses (CNWRA®) to conduct a literature review and independent analyses of the corrosion behavior of copper and carbon steel waste package materials in anoxic environment.

The specific objectives of this work were to:  (i) confirm the low uniform corrosion rates reported in the literature for copper and carbon steel because corrosion rate is an important parameter to predict waste package lifetime, (ii) evaluate hydrogen generation and hydrogen absorption accompanying corrosion of copper and carbon steel because the accumulation of hydrogen in the repository could affect the disposal environment and ultimately other processes such as spent fuel dissolution, and (iii) study the effect of chloride, sulfide, and thiosulfate on passive dissolution of carbon steel because passivity is important to understand waste package material long term performance.

Examination of literature data shows that the constant corrosion rates for carbon steel in anoxic environments ranged from 0.1 to 10 μm/yr [0.004 to 0.39 mils/yr], with pitting corrosion in the same rate as general corrosion over long term periods.  This corrosion behavior was implemented in the NRC and CNWRA jointly developed generic performance assessment model.  Recent literature shows that carbon steel remained passive in simulated concrete pore water under anoxic conditions and the passive oxide film behaved like an n-type semiconducting oxide film consisting of two layers:  (i) inner barrier layer and (ii) outer precipitated layer.  In anoxic conditions, general corrosion of carbon steel leads to hydrogen gas generation at the waste container/buffer interface.  Although carbon steel has been reported to remain passive in alkaline water, it has been shown to exhibit active behavior when in contact with compacted bentonite where sulfide, chloride, and thiosulfate in hundreds of ppm level could be present.  According to the literature, the main uncertainties arise from the corrosion rate determining the container failure time and the impacts of corrosion products [i.e., $H_2$ and Fe(II)], on the properties of other barriers in the multibarrier system.

Experimental studies were conducted on carbon steel to examine uncertainties associated with processes and models for an alkaline reducing environment, which could occur in the presence of a concrete overpack.  Weight loss and electrochemical tests have confirmed low uniform corrosion rates of carbon steel in an alkaline reducing environment at a pH of about 12.  Immersion tests in an autoclave under reducing conditions show that a very small amount of hydrogen production accompanied the passive dissolution process.  Polarization tests over a range of potentials show that chloride had the least depassivation effect and sulfide had the most depassivation effect on carbon steel passivity in this alkaline reducing environment.  Thiosulfate was intermediate between these two.  Scratch repassivation tests demonstrated that carbon steel has a strong tendency to repassivate after the oxide film was disrupted by

scratching.  However, chloride-containing alkaline solutions had a tendency to pit the carbon steel material.

Literature data show that the constant corrosion rates for copper in anoxic environments ranged from $4 \times 10^{-3}$ to $2 \times 10^{-2}$ µm/year [$2 \times 10^{-4}$ to $8 \times 10^{-4}$ mils/year], with pitting corrosion occurring at the same rate as general corrosion over long term periods.  This corrosion behavior was also implemented in the NRC and CNWRA jointly developed generic performance assessment model.  Within the literature there is controversy over the copper corrosion rate in anoxic water depending on the proposed corrosion mechanism.  Based on thermodynamic modeling and Pourbaix diagrams, copper waste containers of thickness 5 cm [2 in] will maintain their integrity for nuclear waste containment up to 100,000 years.  However, considering formation of a thermodynamically more favorable solid phase from copper dissolution, a more than 1 m [39 in] copper thickness might be required for 100,000-year durability.  According to the literature, the main uncertainties arise from thermodynamic stability of copper in anoxic pure water, copper sulfide film passivity in sulfide-containing environment, and damage accumulation during the repository unsaturated period.

Experimental tests of general corrosion and hydrogen generation for copper samples were conducted by CNWRA under anoxic conditions with $O_2$ concentration less than 10 ppb using a saline synthetic groundwater based on reference compositions for deep groundwaters in crystalline rocks of the Canadian Shield.  Results from CNWRA experimental tests have indicated that copper corrosion rates measured with electrochemical linear polarization and impedance spectroscopy were higher than the predicted values reported in the literature based on thermodynamic calculations at this $O_2$ level without considering the effect of chloride, but they were close to some literature results measured with the same electrochemical method in pure water.  Hydrogen was also found to be generated by the corrosion process, albeit in very small amounts.  This observation differs from statements in the literature that copper would experience little to no corrosion in a reducing environment.  The difference in corrosion rate and hydrogen generation could be caused by different solution and methodology used in this work.  More in-depth analyses are warranted to further understand differences with information in the literature.

# ACKNOWLEDGMENTS

# QUALITY OF DATA, ANALYSES, AND CODE DEVELOPMENT

**DATA**:  The computer software PHREEQCI (USGS, 2003) was used in the analysis of simulated granitic water.  All CNWRA-generated original data contained in this report meet the quality assurance requirements described in the Geosciences and Engineering Division Quality Assurance Manual.  Sources for other data should be consulted for determining the level of quality for those data.  Scientific Notebook 1142 was used (Chiang and He, 2014).

**ANALYSES AND CODES**:  none

**REFERENCE**:

Chiang, K. and X. He.  "Carbon Steel and Copper Corrosion Tests."  Scientific Notebook 1142. San Antonio, Texas:  Center for Nuclear Waste Regulatory Analyses.  pp. 30–91.  2014.

USGS.  "PHREEQCI, v. 2.8."  Reston, Virginia:  United States Geological Survey.  2003.

# 1 INTRODUCTION

## 1.1 Background

Currently, the U.S. Nuclear Regulatory Commission (NRC) is making preparations to support national policy changes for managing the back end of the nuclear fuel cycles.  The Center for Nuclear Waste Regulatory Analyses (CNWRA$^®$) is assisting NRC in identifying and analyzing key regulatory and technical issues associated with high-level waste (HLW) disposal in a variety of potential repository designs and geologic media.  The engineered barrier is typically designed to work with the natural barrier in the repository to isolate the HLW from the biosphere.  Waste packages are one important part of the engineered barrier system.  Waste package materials could undergo chemical degradation (i.e., corrosion) when contacted by groundwater.  Long lifetimes of waste packages could limit radionuclide release to the biosphere.  As such, corrosion of waste packages is an important technical issue in HLW disposal.

Various factors determine the selection of waste package materials including the corrosion behavior in the expected disposal environment.  Most of the proposed underground disposal repositories are located in the saturated zone below the water table, where the amount of $O_2$ available for corrosion is limited to that initially trapped in the repository at closure.  The limited amount of $O_2$ will be consumed by a combination of waste package corrosion, aerobic microbial activity, and the oxidation of some oxidizable minerals in the repository.  The duration of this initial oxidizing period is estimated to range from 1 to 100 years (King, 2010a).  Afterwards, the environment will evolve to anoxic and then to reducing.  A wide range of alloys have been considered as candidate waste package materials for the saturated repositories including copper, carbon steel and cast iron, stainless steels, and titanium alloys (King, et al., 2013).

Recently, NRC and CNWRA jointly developed a generic performance assessment model, named the Scoping of Options and Analyzing Risk (SOAR) to provide risk and performance insights for a variety of potential HLW geologic disposal systems (Markley, et al., 2011).  Five key model components are considered in SOAR:  Waste Form, Waste Package, Near Field, Far Field, and Biosphere.  Three distinct waste forms are considered in the model.  The Waste Package model accounts for chemical degradation due to corrosion of four distinct waste package materials:  copper, carbon steel, titanium, and stainless steel (Jung, et al., 2011; He, et al., 2011).  The near field component models radionuclide transport through the waste package internals, surrounding backfill, and the disturbed zone within the geologic host formation.  The far field model incorporates three independent segments.  System performance is measured in terms of release rates or dose.

Among the candidate waste package materials, carbon steel and copper are being considered as corrosion allowance materials in several countries (King, 2013).  To address some key regulatory and technical issues associated with these two materials, NRC directed CNWRA to conduct a literature review and independent technical analyses of carbon steel and copper in anoxic environments.

## 1.2 Scope and Objectives

This report provides independent analyses of carbon steel and copper waste container materials based on the review of recent literature beyond that reported in Jung, et al. (2011) and the results of new experimental studies conducted by the authors.  The experimental studies for carbon steel have been conducted in anoxic alkaline solutions to simulate an environment in the

presence of a concrete overpack.  Copper corrosion tests were conducted in anoxic simulated granitic water.  The specific objectives of this work are to:

- Confirm the low uniform corrosion rates reported in the literature for copper and carbon steel because corrosion rate is an important parameter to predict the lifetime of waste packages.

- Evaluate hydrogen generation and hydrogen absorption accompanying corrosion of copper and carbon steel because the accumulation of hydrogen in the repository could affect the disposal environment and ultimately affect other processes such as fuel dissolution.

- Study the effect of chloride, sulfide, and thiosulfate on passive dissolution of carbon steel because passivity is important to understand waste package material long term performance.

## 1.3        Organization of the Report

This report is organized into four chapters, beginning with an Introduction and Literature Review of carbon steel and copper as waste package materials in Chapter 1.  Chapters 2 and 3 present the experimental details and data on carbon steel in alkaline water and copper in granitic water, respectively.  Conclusions from the study are provided in Chapter 4.

## 1.4        Review of Carbon Steel Waste Package Corrosion Literature

One advantage of using carbon steel is that the industry has experience with the fabrication and welding of thick-walled carbon steel structures, and the material is relatively inexpensive.  Carbon steel is a corrosion allowance material that is reported to be passive in alkaline pore water and it can also provide some mechanical strength.  It has been selected as a candidate canister material in several countries, including Switzerland, France, Belgium, Japan, and Canada, for underground geologic disposal of HLW where an anoxic to reducing environment dominates after the thermal period.  It is reported to have low corrosion rates (several micrometers per year) in simulated reducing groundwater, which makes it possible to last for thousands of years.

The supercontainer concept as the waste package design in Belgium's proposed Boom Clay repository comprises an inner carbon steel overpack containing the waste and an outer stainless steel liner.  The annulus between the carbon steel overpack and stainless steel liner is filled with a cementitious material.  The outer surface of the carbon steel overpack is expected to be in contact with concrete porewater with pH about 12.5 persisting for thousands of years, in which passive dissolution is predicted to be the dominant corrosion mode and other degradation modes such as pitting corrosion and microbially influenced corrosion can be excluded (Kursten, et al., 2011; King, 2007, 2010b).  Under passive dissolution, a ferrous hydroxide film was reported to form on the metal surface at low temperatures {30 °C [86 °F]}, with magnetite ($Fe_3O_4$) film forming at higher temperatures {50 and 80 °C [122 and 176 °F]}.  The long-term anaerobic corrosion rate of carbon steel in alkaline media is estimated to be on the order of 0.12 and 1 $\mu$m/yr [0.0047 and 0.04 mils/yr] at 30 and 80 °C [86 and 176 °F], respectively.  Chloride ions were found to have little effect on the corrosion rate, but calcium ions were found to improve the protectiveness of the film.  A depassivation effect of $S^{2-}$ and $S_2O_3^{2-}$ on the film has also been reported (Kursten, et al., 2011).

In anoxic conditions after the thermal period, general corrosion of carbon steel will lead to hydrogen gas generation at the waste container/buffer interface via the reaction

$$Fe + 2H_2O \Leftrightarrow Fe(OH)_2 + H_2 \tag{1-1}$$

Under this condition, $Fe(OH)_2$ may decompose, forming magnetite through the following reaction

$$3Fe(OH)_2 \Leftrightarrow Fe_3O_4 + 2 H_2O + H_2 \tag{1-2}$$
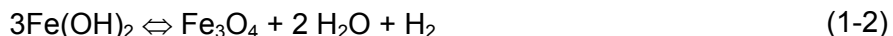
Some of the hydrogen could be absorbed into the material. The susceptibility to hydrogen embrittlement or hydrogen-induced cracking in carbon steel will depend on the type of steel and the specific environmental conditions.

Based on examination of literature data, constant corrosion rates for carbon steel in anoxic environments used in SOAR (Jung, et al., 2011) were estimated to be 0.1 to 10 µm/year [0.004 to 0.39 mils/yr]. Lu, et al. (2013), Macdonald, et al. (2013), and Urquidi-Macdonald, et al. (2013) have shown that carbon steel remains passive in simulated concrete pore water [$Ca(OH)_2$ + 0.3 M NaOH + 0.1 M NaCl] under anoxic conditions and the passive oxide film behaves like an n-type semiconducting oxide film. Urquidi-Macdonald, et al. (2013) indicated the passive film consists of two layers: (i) inner barrier layer and (ii) outer precipitated layer. Smart, et al. (2013) found that the corrosion rate of carbon steel in alkaline simulated porewater decreases with time, which is consistent with the formation of a thin barrier oxide layer and a thicker outer layer composed of precipitated magnetite. Furthermore, they found that irradiation of the specimen at 23–25 Gy hr$^{-1}$ did not increase the corrosion rate.

Although carbon steel is reported to remain passive in alkaline water, it has been shown to exhibit active behavior in contact with compacted bentonite (King, 2013) where sulfide, chloride, and thiosulfate in hundreds of ppm level could be present (Kursten, et al., 2011). Newman, et al. (2013), detected hydrogen generated from carbon steel corrosion in cementitious grout under anoxic conditions. The corrosion rate correlated to hydrogen gas generation was found to be less than 1 nm/yr [$4 \times 10^{-5}$ mils/yr]. In alkaline concrete pore water, the primary corrosion product is $Fe_3O_4$ and corrosion rates are on the order of 0.1 µm/yr [0.004 mils/yr] (Kursten, et al., 2013), but carbon steel could still be susceptible to localized corrosion. King (2013) commented that the main area of current interest for carbon steel is its anaerobic corrosion for high-level waste containment applications. Uncertainties arise from the actual corrosion rate that is used to determine the container failure time and the impacts of corrosion products [e.g., $H_2$ and Fe(II)] on the properties of other components in the disposal system.

## 1.5    Review of Copper Waste Package Corrosion Literature

Copper has been proposed for use as a waste package material in several repository programs including those in Switzerland, Sweden, Finland, Japan, and Canada (King, 2013). Copper tends to corrode uniformly in Cl$^-$ containing environments with little tendency to exhibit localized corrosion or stress corrosion cracking, which is the advantage of copper over other materials. According to the copper Pourbaix (potential-pH) diagram (Pourbaix, 1974) in anoxic environments, copper is thermodynamically stable and corrosion represented by Reaction (1-3) would be negligible

$$2Cu + H_2O \Leftrightarrow Cu_2O + H_2 \tag{1-3}$$
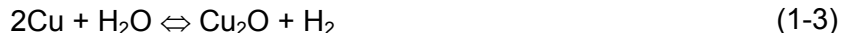
Because of the negligible corrosion in anoxic water, copper containers could be extremely long-lived for a wide range of host rock types. However, partly because of the susceptibility to microbially influenced corrosion and its high maleability, copper is usually designed to be used in conjunction with a buffer material and with an insert of carbon steel for mechanical support. Based on examination of literature data, the constant corrosion rates for copper in anoxic environments used in SOAR (Jung, et al., 2011) were estimated to be $4 \times 10^{-3}$ to $2 \times 10^{-2}$ μm/yr [$2 \times 10^{-4}$ to $8 \times 10^{-4}$ mils/yr], with a pitting enhancement factor of 1.0, which means that pitting corrosion is assumed to occur at the same rate as general corrosion under this environment.

Copper is the material of choice for the waste container in the Swedish Nuclear Fuel Company's license application for long term disposal of spent nuclear fuel. The corrosion rate is based on modeling (e.g., Pourbaix diagrams and thermodynamic data) with a corrosion rate of $5 \times 10^{-5}$–0.02 μm/yr [$2 \times 10^{-6}$–$8 \times 10^{-4}$ mils/yr] (Roseborg and Werme, 2008). According to the model, a copper waste container of thickness 5 cm [2 in] will maintain its integrity for nuclear waste containment up to 100,000 years. However, Hultquist, et al. (2009) proposed a solid phase of $H_xCuO_y$ (equivalent to CuOH for x = y = 1) as the corrosion product, which is different from $Cu_2O$ in Reaction (1-3). Through this different corrosion mechanism, the equilibrium hydrogen partial pressure and the extent of corrosion will be much higher. More than 1 m [39 in] of copper thickness might be required for 100,000 years durability. Scully and Hicks (2012) conducted a review for the Swedish Radiation Safety Authority and recommended further work to resolve the controversy over the corrosion mechanisms in anoxic water. However, King (2013) stated that the consequence of alternative phase formation is low because the corrosion rate will eventually be limited by the accumulation of hydrogen in the repository if copper corrosion proceeds through the following simplified reaction:

$$2Cu + 2H_2O \rightarrow 2CuOH + H_2 \tag{1-4}$$

Overall, King (2013) commented that although there has been considerable work on the corrosion behavior of copper relevant to repository environments, the following are three main issues that are still being actively investigated:

1.    Thermodynamic stability of copper in anoxic pure water
2.    Copper sulfide film passivity in sulfide-containing environment
3.    Damage accumulation during the repository unsaturated period

The work conducted under the current project aimed at gaining an independent understanding on the first issue on copper corrosion in anoxic water.

# 2 CARBON STEEL CORROSION EXPERIMENTS IN ALKALINE WATER

## 2.1 Experimental Approaches

### 2.1.1 Material and Solutions

Material used in the test is the commonly used carbon steel A516 Grade 60 (ASTM International, 2010, ASTM A516/ 516M–10). The chemical composition from independent analysis is shown in Table 2-1.

The solution used is an anaerobic alkaline solution simulating concrete pore water, which was prepared with saturated $Ca(OH)_2$, without adjustment of pH. The anaerobic condition was achieved by deaerating the solution before and during the test with ultrahigh purity (UHP) argon. In some tests, $Cl^-$, $S_2O_3^{2-}$, and $S^{2-}$ were added into the $Ca(OH)_2$ solution to observe the effect of these species on passivity of carbon steel.

### 2.1.2 Corrosion Rate Measurement

Weight loss, electrochemical impedance spectroscopy (EIS), and linear polarization resistance (LPR) were used to measure corrosion rates of carbon steel exposed to deaerated solutions at 50 and 80 °C [122 and 176 °F]. Weight loss measurements provide an average corrosion rate over the testing period, while EIS or LPR provides instantaneous corrosion rates. All the techniques are complementary and were used in this study to estimate the corrosion rates with higher degree of confidence.

Small coupons with approximate dimensions of $1 \times 2 \times 0.2$ cm [$0.4 \times 0.8 \times 0.08$ in] were used for weight loss analysis and a cylindrical specimen 6.4 mm [0.25 in] in diameter and 50 mm [2 in] in length was used for open circuit potential (OCP) and EIS measurements over time. EIS measurements were made using a potentiostat coupled to a frequency response analyzer (FRA) in a glass cell with argon deaeration. Prior to each EIS measurement, the electrode was held at its OCP for at least seven days. Based on the features of the EIS data, the simplest and most common circuit—the Randles circuit shown in Figure 2-1 and consisting of a solution resistance ($R_s$), a double layer capacitance ($C_{dl}$), and a charge transfer or polarization resistance ($R_p$)—was used as a starting point to analyze the EIS data to obtain $R_p$. LPR was performed between −10 to 10 mV versus OCP. The LPR data was fit linearly to obtain $R_p$. The corrosion rate was calculated in accordance with ASTM G102 from $R_p$ measured from both EIS and LPR and Eqs. (2-1) and (2-2) below (ASTM International, 2004). The Stearn-Geary constant, B, in Eq. (2-1) is a constant to correlate corrosion current density, $i_{corr}$, to $R_p$ in the linear polarization region. The constant depends on the Tafel slopes of anodic and cathodic reaction. In this study, the constant considered is 0.027 V, assuming that both the anodic and cathodic Tafel slopes are 0.12 V.

$$i_{corr} = \frac{B}{R_p} \tag{2-1}$$

$$\text{Corrosion Rate (mm/yr)} = \frac{K\, i_{corr}\, EW}{\rho} \tag{2-2}$$

where

$i_{corr}$   =   corrosion current density (A/cm$^2$)
B      =   Stearn-Geary Constant (0.027 V assumed)

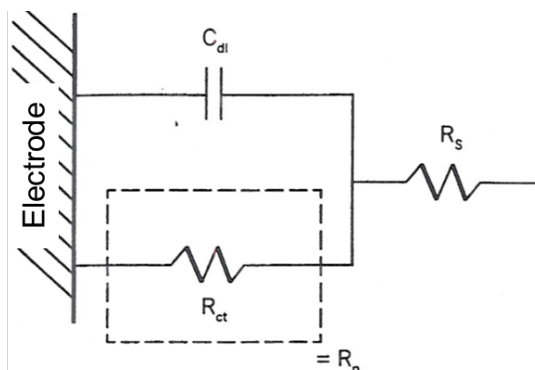| Table 2-1.  Chemical Composition of A516 Grade 60 Carbon Steel (wt%) | | | | | | | | | |
|---|---|---|---|---|---|---|---|---|---|
| C | S | Mn | P | Si | Cr | Mo | Al | V | Fe |
| 0.18 | 0.011 | 0.90 | 0.011 | 0.30 | 0.02 | <0.01 | 0.021 | <0.01 | Balance |
| C = carbon, S = sulfur, Mn = manganese, P = phosphorus, Si = silicon, Cr = chromium, Mo = molybdenum, Al = aluminum, V = vanadium, Fe = iron | | | | | | | | | |



**Figure 2-1.  Randles Circuit Used As a Starting Point to Fit the EIS Data [$C_{dl}$—Double Layer Capacitance; $R_{ct}$—Charge Transfer Resistance; $R_p$—Polarization Resistance; $R_s$—Solution Resistance**

$R_p$   =   polarization resistance ($\Omega \cdot cm^2$)
K      =   constant equal to $3.27 \times 10^3$ mm g/(A cm yr) for carbon steel to compute corrosion rates in mm/yr units when the density is in g/cm$^3$ units and the equivalent weight is in g units.
$\rho$   =   density in g/cm$^3$ {7.86 g/cm$^3$ [0.283 lb/in$^3$] for carbon steel}
EW     =   material equivalent weight in grams/equivalent weight {27.9 g [0.977 oz] for carbon steel}

## 2.1.3      Hydrogen Generation Measurement

Hydrogen generated from the corrosion process was collected and the concentration was quantified to determine the extent of hydrogen production.  Carbon steel coupons with dimensions of 3.2- × 25- × 75-mm [0.12- × 1.0- × 3.0-in] were used in the tests.  The coupons were polished up to 600 grit sand paper before exposure and the actual dimensions were measured before the test.  In each test, six coupons were exposed to the Ca(OH)$_2$ solution in an autoclave maintained at 80 °C [176 °F].  The total surface area of all the coupons was approximately 250 cm$^2$ [38.8 in$^2$].  The autoclave cylinder and head were made from Hastelloy® (one nickel-based super alloy) and Type 316 stainless steel, respectively.  There is a Teflon liner inside the cylinder to avoid direct solution contact with the cylinder.  The autoclave has a pressure rating of 136 atm [2,000 psi].  A Teflon® gasket with temperature rating of 250 °C [482 °F] provided the seal between the pressure vessel body and the lid, which were held together with a split-ring clamp and drop band.  The pressure vessel lid was fitted with a thermocouple well and a calibrated pressure gauge for temperature and pressure monitoring.  A needle valve for gas sampling and a pressure relief valve were connected to the autoclave.

The volume of the autoclave was 2.1 L [0.55 gal] and the solution amount was 1.2 L [0.32 gal], which gives 0.9 L [0.24 gal] vapor space.  The solution was deaerated with UHP argon gas in a

UHP nitrogen gas purged glove box. In the process of deaeration, the oxygen concentration was measured with an oxygen meter with resolution of 10 ppb. After both the oxygen concentration in the solution and the glove box were below the detection limit of the oxygen meter, the autoclave was sealed in the glove box to achieve anaerobic conditions. Figure 2-2 shows one photo of the autoclave with the vessel in the heater to achieve the desired temperature. Assuming that the oxygen concentration is 10 ppb after sealing the autoclave, the oxygen amount is calculated to be only $9 \times 10^{-10}$ mol. If this amount of oxygen reacts with carbon steel in the following reaction, Eq. (2-3):

$$2Fe + O_2 + 2H_2O \rightarrow 2Fe(OH)_2 \qquad\qquad (2\text{-}3)$$

the amount of iron consumed by the oxygen is $2 \times 10^{-9}$ mol. Using total surface area of 250 cm$^2$ [38.8 in$^2$] and carbon steel density of 7.86 g/cm$^3$ [0.283 lb/in$^3$], $5 \times 10^{-4}$ nm [$2 \times 10^{-8}$ mils] of carbon steel layer would be consumed by the residual 10 ppb oxygen. This suggests that the effect of this residual oxygen is negligible.

The gas from the vapor phase was sampled at 3 and 6 months using Tedlar® gas sampling bags and analyzed with gas chromatography immediately after sampling. The gas chromatography instrument used has a hydrogen detection limit of 0.01 volume percent. Before each measurement, the instrument was calibrated with hydrogen-nitrogen mixtures with known hydrogen contents of 0.01, 0.05, and 0.25 volume percent. The posttest metal coupons were cut for hydrogen analysis in the metal.

### 2.1.4    Scratch Repassivation Test

The scratch repassivation test investigated the repassivation capability of carbon steel passive film when it was mechanically disrupted by scratching the metal surface. A cell shown in Figure 2-3(a) was set up to measure the repassivation current of the carbon steel working electrode samples after a surface scratch was made while the electrode was polarized at −300, −200, −100, 0, 100, 200, 300, 400, and 500 mV versus saturated calomel electrode (SCE), respectively. The working electrode was a hollow cylindrical shaped specimen. The height, outer diameter, and inner diameter of the working electrode were 1.0 cm [0.39 in], 1.2 cm [0.47 in], and 0.64 cm [0.25 in], respectively. The working electrode potentials were measured with respect to the saturated calomel reference electrode. A platinum mesh was used as a counter electrode. All tests were conducted at 50 °C [122 °F]. The test solution was deaerated with UHP argon gas. A cartridge heater sheathed in a glass thermowell was used to heat up the solution. In each test, 2 L [0.55 gal] Ca(OH)$_2$ solution was used. The scratch on the carbon steel working electrode shown in Figure 2-3(b) was made by impinging a diamond tip loaded on a stainless steel rod into a working electrode rotating at 30 revolutions per minute for 2 seconds; as such, one scratch was one complete revolution around the surface (i.e., 30/60 × 2). Two minutes after one scratch was made, another scratch was made at the same location. This process was repeated at another location on the same sample by shifting the sample vertically for each test specimen. Figure 2-3(b) shows the scratch process as an example.
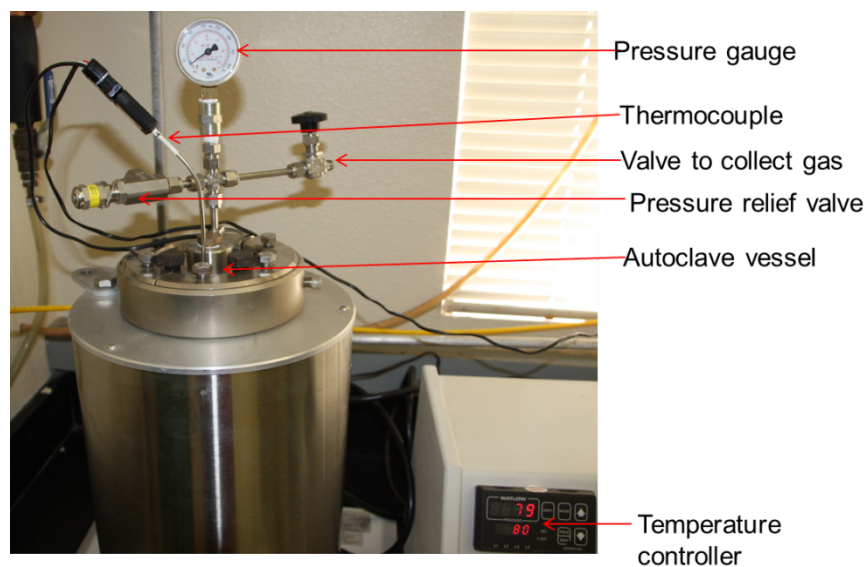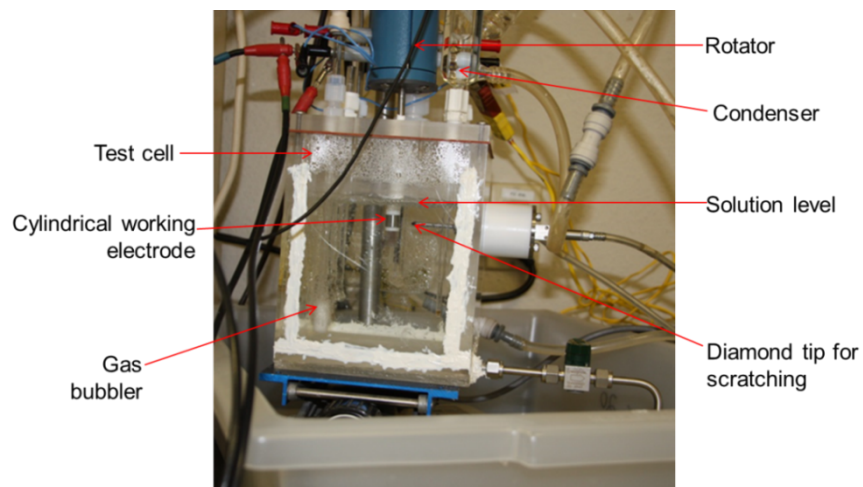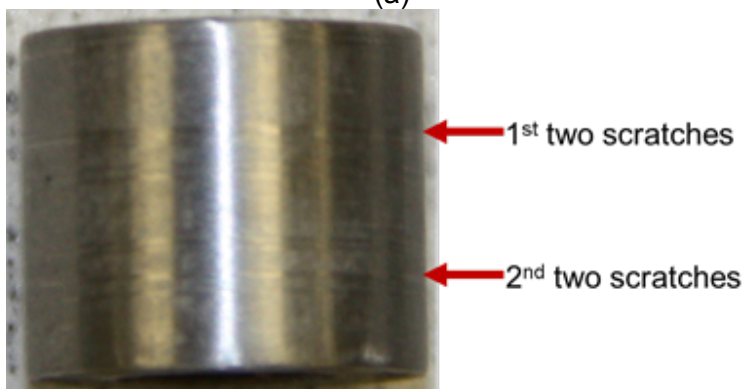
**Figure 2-2. Autoclave for Hydrogen Generation Measurement**



(a)



(b)

**Figure 2-3. (a) Scratch Repassivation Test Cell and (b) Example of Scratches on the Working Electrode**

## 2.2        Results

### 2.2.1        Corrosion Rate from Immersion Tests

Carbon steel specimens were immersed in alkaline $Ca(OH)_2$ solution at 50 °C [122 °F] for 6 months and at 80 °C [176 °F] for 3, 6, 9, and 12 months.  Figure 2-4 shows some posttest specimens.  Some areas of the samples were covered by a black film, which is possibly $Fe_3O_4$. Examination under the microscope shows there is some pitting in the specimens.  Examples of pits are shown in Figure 2-4.  Corrosion rates were calculated from the weight loss data and summarized in Table 2-2.  The 6-month average corrosion rates at 50 and 80 °C [122 and 176 °F] were 0.092 and 0.17 µm/yr [0.0037 and 0.0066 mils/yr], respectively.  The corrosion rate at 50 °C [122 °F] was lower than measured at 80 °C [176 °F] at the same time duration.  For tests at 80 °C [176 °F], the 3-month corrosion rate was almost one order of magnitude higher than those at longer durations.  This suggests the material may have experienced higher corrosion rates immediately after immersion.  However, there is no clear trend of corrosion rate decreasing with time from 6 to 12 months.

### 2.2.2        OCP and EIS Measurement

A cylindrical specimen with outer diameter 6.4 mm [0.25 in] and length 50 mm [2.0 in] was used for OCP and EIS measurements.  EIS was measured weekly.  OCP was monitored while EIS was not measured.  The exposure time was about 6 and 4 months respectively at 50 and 80 °C [122 and 176 °F].  OCP data measured at 50 and 80 °C [122 and 176 °F] are shown in Figure 2-5 and some of the EIS data displayed in both Nyquist and Bode plots are shown in Figure 2-6.  OCP shifted from −0.37 to −0.25 $V_{SCE}$ at both temperatures and they fluctuated with time.  The OCP is close to the model prediction by Kursten, et al. (2011) at the end of the transition phase and the beginning of the anoxic phase.

EIS data showed only one time constant.  The increasing impedance with decreasing frequency and the near constant phase angle indicated passivity of the surface oxide film over a wide frequency range.  The data showing one time constant was fit well with the Randles circuit in Figure 2-1.  Longer time EIS data at 50 °C [122 °F] indicated presence of another time constant (Data are not shown in Figure 2-6).  The data could not be adequately fitted to the one-time constant electrical circuit because of the difference in the number of time constants.  This indicated that there was some passivity loss and repair events while the electrode was exposed to the solution.  Further analysis is needed to understand the phenomenon better.  The polarization resistance, $R_p$, obtained from the circuit model, was used to calculate corrosion rate based on Eqs. (2-1) and (2-2).  The corrosion rates are summarized in Table 2-3.  At 50 °C [122 °F], the higher corrosion rates measured at later times by EIS corresponded to the higher uncertainty in fitting the EIS data to the one-time constant electrical circuit, which also led to higher corrosion rates at 50 °C than at 80 °C.  The corrosion rates in Table 2-3 were in the range of 0.1 to 3 µm/yr [0.004 to 0.1 mils/yr], which were close to the range of 0.02 to 1.5 µm/yr [0.0008 to 0.06 mils/yr] listed in Table 2-2.
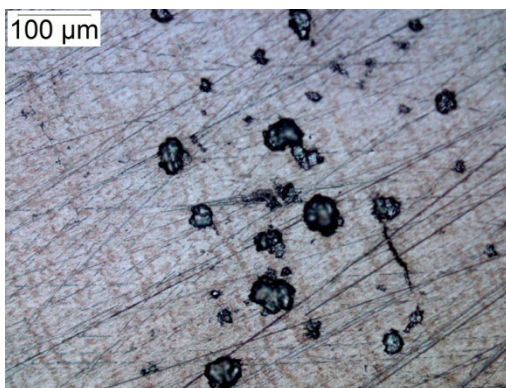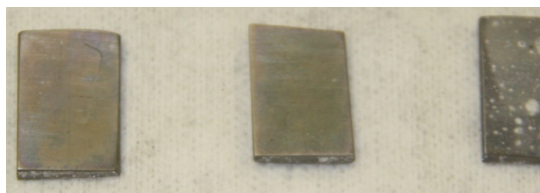
(a)
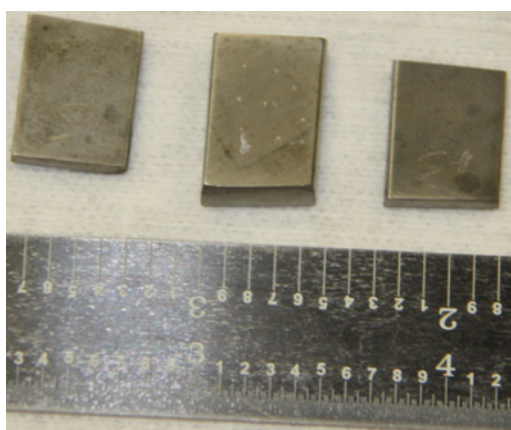


(b)

**Figure 2-4.  Carbon Steel Specimens Exposed to Deaerated Ca(OH)$_2$ for 6 Months at (a) 50 °C [122 °F] and (b) 80 °C [176 °F]**

| Table 2-2.  Corrosion Rates of Carbon Steel Exposed to Ca(OH)$_2$ at 50 and 80 °C [122 and 176 °F] Measured by Weight Loss Coupons | | | | | | |
|---|---|---|---|---|---|---|
| **Tests** | | **50 °C [122 °F] for 6 months** | **80 °C [176 °F]** | | | |
| | | | **3 months** | **6 months** | **9 months** | **12 months** |
| Corrosion rate (µm/yr) | Individual | 0.077, 0.056, 0.142 | 1.16, 1.42 | 0.33, 0.022, 0.16 | 0.35 0.23 | 1.41* 0.12 0.24 0.13 |
| | Average | 0.092 ± 0.045 | 1.29 ± 0.13 | 0.17 ± 0.15 | 0.29 ± 0.09 | 0.16 ± 0.07 |
| *This value was treated as an outlier in the calculation for average. | | | | | | |
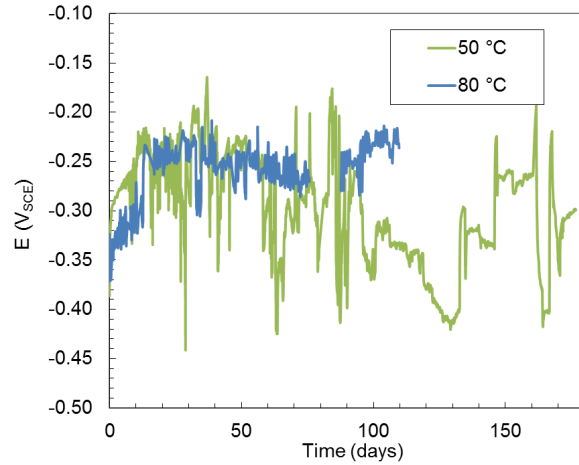
**Figure 2-5. OCP of Carbon Steel Specimens Exposed to Deaerated Ca(OH)₂ at 50 °C and 80 °C [122 and 176 °F]**



(a)



(b)
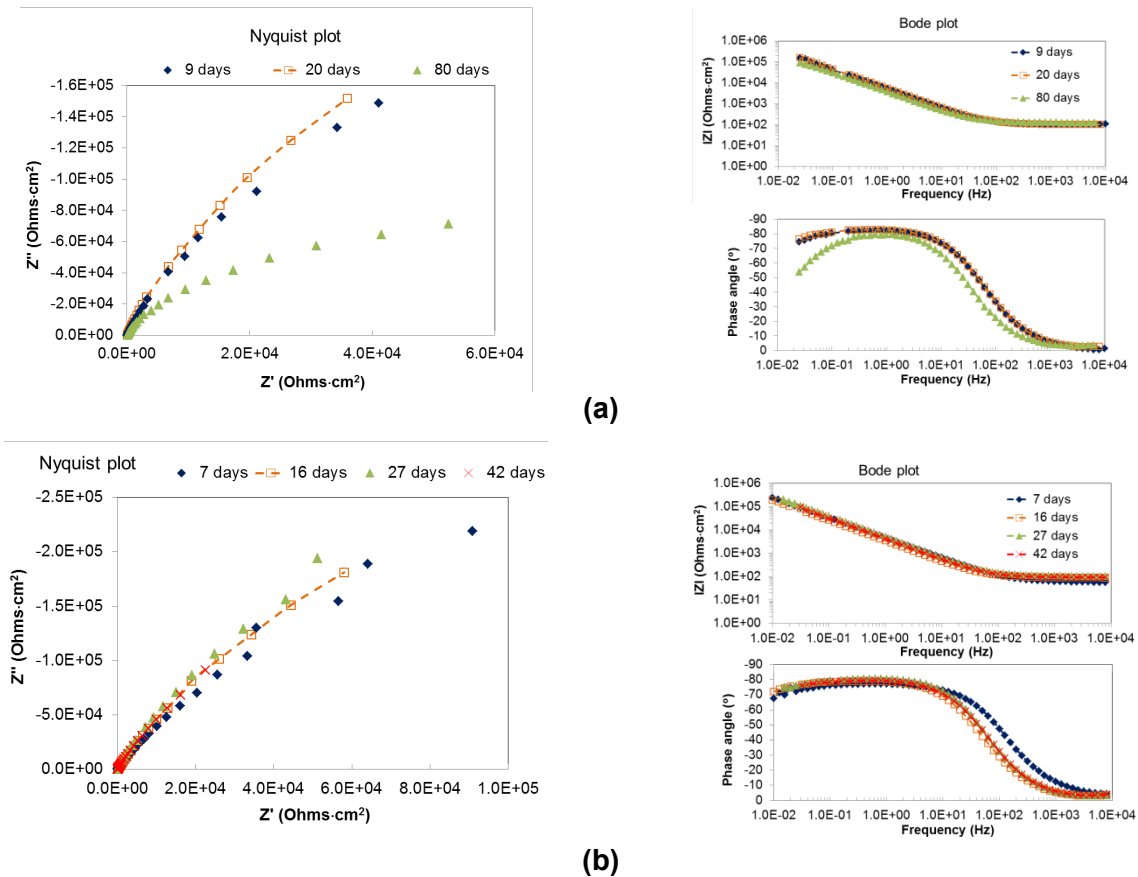
**Figure 2-6. EIS Nyquist and Bode Plots of Carbon Steel Specimens Exposed to Deaerated Ca(OH)₂ at (a) 50 °C [122 °F] and (b) 80 °C [176 °F].**
**In the Nyquist Plot, x and y-axes are the real and imaginary components, respectively, of the impedance. In the Bode Plot, the x-axis is the frequency and the y-axis is the amplitude of the impedance in the top plot and phase angle in the bottom plot.**

| Table 2-3. Corrosion Rates of Carbon Steel Exposed to $Ca(OH)_2$ at 50 and 80 °C [122 and 176 °F] Measured by EIS and Linear Polarization Methods | | | |
|---|---|---|---|
| 50 °C [122 °F] | Corrosion rate, µm/yr | Time Duration | 1—26 Weeks |
| | | Individual | 0.30, 0.10, 0.26, 0.12, 1.45, 1.60, 2.77, 1.39, 0.29* |
| | | Average | 0.92 ± 0.67 |
| 80 °C [176 °F] | Corrosion rate, µm/yr | Time Duration | 1—6 Weeks |
| | | Individual | 0.23, 0.22, 0.22, 0.16 |
| | | Average | 0.21 ± 0.03 |
| *By linear polarization resistance method | | | |

### 2.2.3        Hydrogen Generation Analysis

With the heating up of the autoclave, the internal pressure increased.  After the autoclave temperature was stabilized at 80 °C [176 °F], the pressure remained steady at 0.47 atm [7 psi].  The pressure increase corresponding to the temperature is primarily from two sources:  (i) the pressure of the nitrogen gas contained in the autoclave originally at 1 atm [14.7 psi] increased with increasing temperature and (ii) water evaporates.  Using the ideal gas law and the 0.9 L [0.24 gal] head space, the pressure increase from 20 to 80 °C [68 to 176 °F] is 0.2 atm [2.9 psi], which is lower than the total pressure increase.  This means that water also evaporated into the head space at this temperature, which led to a pressure increase of 0.27 atm [4.0 psi].  The relative humidity in the autoclave was calculated to be 57 percent using a water vapor pressure of 0.47 atm [7 psi] (Hardy, 1998) at the test temperature.  At this relative humidity, corrosion of the stainless steel head and nickel alloy vessel should be negligible and does not contribute to hydrogen generation.

After exposing the carbon steel specimens at 80 °C [176 °F] for 3 months, the valve was opened to collect the gas in the vapor phase until the gauge pressure dropped to zero.  When the valve was opened, the gas expanded to equilibrate with the atmosphere.  After the valve of the gas sampling bag was closed and while the bag was still connected to the autoclave valve, the autoclave valve was closed to prevent air entry into the autoclave.  After the sampled gas cooled down to room temperature, condensed water was observed in the sampling bag, confirming that water evaporated into the head space.  The amount of hydrogen gas detected from the autoclave was below the detection limit of gas chromatography of 0.01 vol%.  After the 1st sampling, the autoclave pressure didn't return to the original value because some gas in the head space was emitted during the 3-month sampling.  UHP nitrogen gas was added to bring the pressure to the same level as before sampling.  The test continued for another 3 months and the gas sample was collected again.  The hydrogen concentration at 6 months was 0.078 volume percent.  The test was repeated under the same conditions and the hydrogen was at 0.101 volume percent at 3 months.  By assuming that corrosion of 1 mole of Fe releases two moles of electrons (i.e., generates 1 mole of $H_2$; Eq. 1-1) and that all the hydrogen gas generated from the corrosion reaction was released to the vapor phase, the estimated corrosion rates were 0.033 and 0.042 µm/yr [0.0013 and 0.0016 mils/yr], which are lower than those measured from weight loss and EIS (Tables 2-2 and 2-3).  This could be because some hydrogen was absorbed into the material.

The test was stopped at 6 months and the autoclave was opened.  The posttest solution and coupons are shown in Figure 2-7.  The solution shown in Figure 2-7(a) remained clear and there was no indication of rust formation, indicating that the anaerobic condition was maintained.  The

coupons shown in Figure 2-7(b) were covered with a grey to black film, possibly $Fe_3O_4$, which is consistent with reported carbon steel corrosion products formed under anaerobic conditions. Microscopic observation shows minor pitting on the specimen, as shown in Figure 2-7(c).

Three types of specimens were analyzed for hydrogen content along with one blank (not-tested) specimen: (i) specimen split into half horizontally without any surface treatment [Figure 2-7(b)], (ii) posttest specimen without any treatment, and (iii) specimen with surface layer removed. The hydrogen contents are summarized in Table 2-4. The Type 1 specimen showed the highest hydrogen content, followed by the posttest specimen without any treatment. This observation suggests that some hydrogen was absorbed into the metal and mostly deposited close to the surface.

### 2.2.4 Effects of Chloride, Thiosulfate, and Sulfide on Passivity and Corrosion Rate

Tests were conducted in deaerated $Ca(OH)_2$ solution with the addition of 100 ppm $Cl^-$, 100 ppm $S_2O_3^{2-}$, 100 and 500 ppm $S^{2-}$ at 80 °C [176 °F]. The specimen was exposed to the solution for one week, then linear polarization and a potentiodynamic scan were performed to determine the effect of these species on corrosion rate and passivity of carbon steel. The open circuit potential and potentiodynamic polarization results are shown in Figures 2-8(a) and (b), respectively. The polarization results show the addition of $Cl^-$, $S_2O_3^{2-}$, and $S^{2-}$ increased the passive dissolution current and there is an active carbon steel dissolution peak at approximately 0 $mV_{SCE}$ for all tests. The passive dissolution current is the lowest with the addition of $Cl^-$ and highest with $S^{2-}$. The effect of $S_2O_3^{2-}$ addition is intermediate between these two. With increasing $S^{2-}$ to 500 ppm, the OCP decreased and the passive dissolution current increased.

Tests also were performed to observe the combined effect of $Cl^-$, $S_2O_3^{2-}$, and $S^{2-}$ on carbon steel passivity. Figures 2-8(c) and (d) show the comparison of OCP and potentiodynamic scan of carbon steel in $Ca(OH)_2$ with the addition of both 100 ppm $Cl^-$ and $S^{2-}$, separately and combined at 80 °C [176 °F]. Both OCP and polarization behavior are close to those with the addition of $S^{2-}$, which has greater effect on passivity than $Cl^-$.

The corrosion rate was determined from linear polarization and summarized in Table 2-5. The corrosion rate increased after the addition of chloride, thiosulfate, and sulfide and the extent of increase increased from chloride, thiosulfate, and sulfide. This set of tests shows that chloride increased the passive dissolution current the least and sulfide increased it the most. Thiosulfate was intermediate between these two.

### 2.2.5 Effects of Applied Potential and $Cl^-$, $S_2O_3^{2-}$, and $S^{2-}$ Addition on Repassivation Behavior from Scratch Tests

Figures 2-9(a), (c), and (e) show the current versus time transient curves for carbon steel when four successive scratches were made at two locations on the surface of the rotating working electrodes at applied potentials of 0, 0.2, and 0.3 $V_{SCE}$ in deaerated $Ca(OH)_2$ solution without and with the addition of $Cl^-$, $S_2O_3^{2-}$, and $S^{2-}$, respectively, at 80 °C [176 °F]. Tests also were performed at other polarization potentials from above the OCP to 0.5 $V_{SCE}$ at 0.1 V interval.
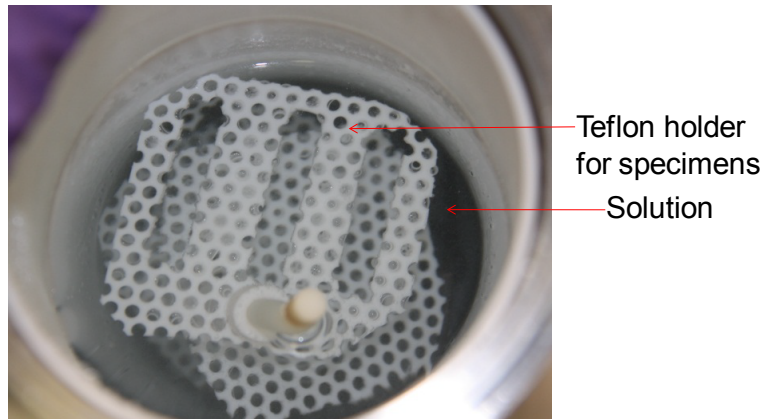
(a)
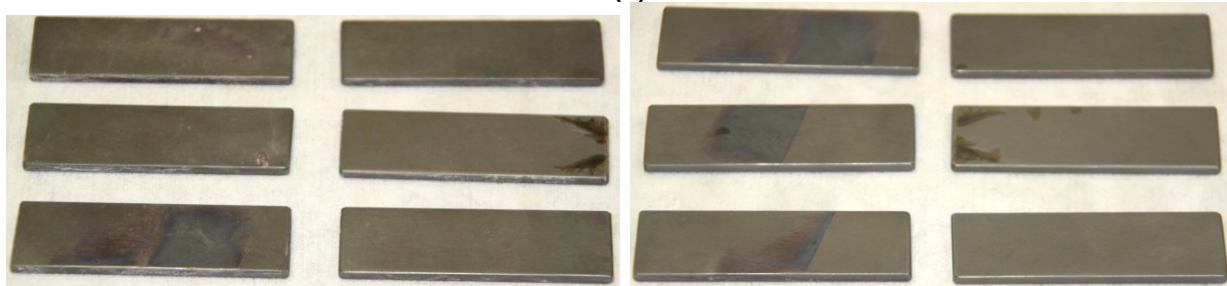


(b)
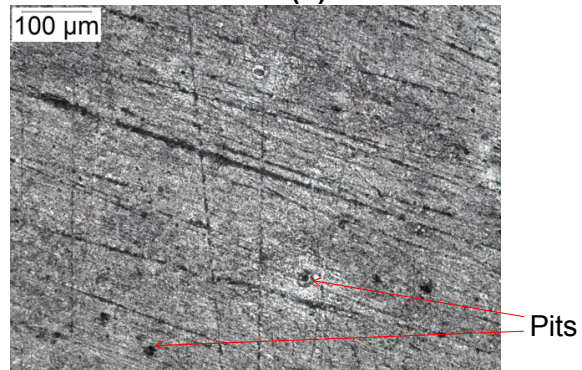


(c)

**Figure 2-7. Carbon Steel Coupons Retrieved From Autoclave After 6 Month Test in Anaerobic Ca(OH)$_2$ Solution at 80 °C [176 °F] (a) Posttest Cell With Solution, (b) Coupons, and (c) Coupons Showing Pits**

| Table 2-4. Hydrogen Content in Carbon Steel Specimens | | | | |
|---|---|---|---|---|
| | 1$^{st}$ type: Specimen split into half horizontally without any surface treatment | 2$^{nd}$ type: Posttest specimen without any treatment | 3$^{rd}$ type: Specimen with surface layer removed | Not-tested specimen |
| Hydrogen content, ppm | 5, 5, 5, 3 | 3, 3 | <1 | 1 |
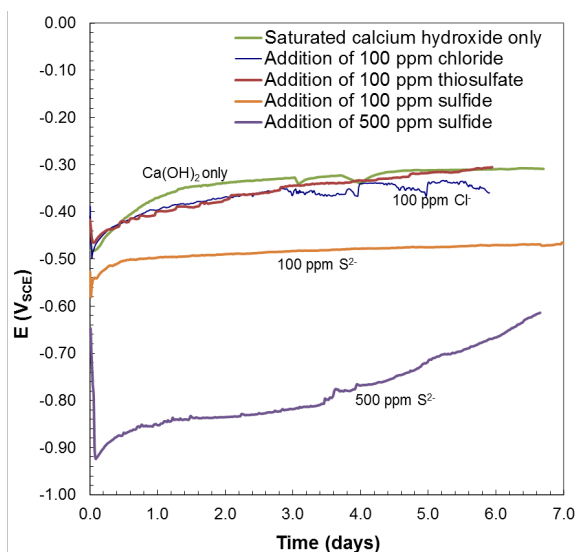
**(a)**
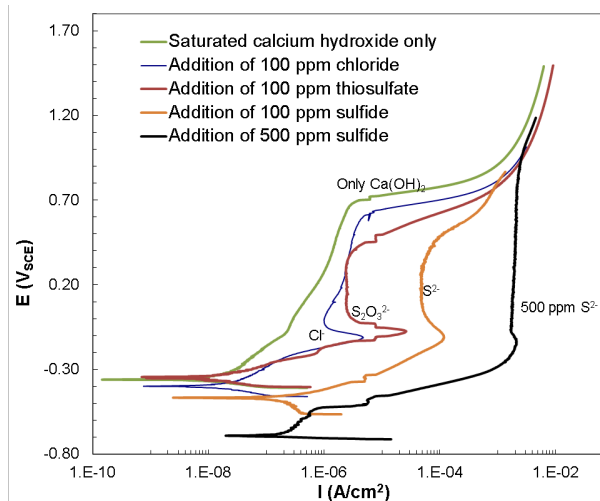
**(b)**
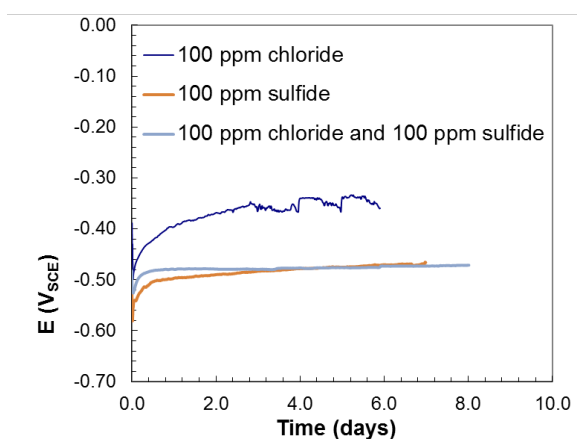
**(c)**
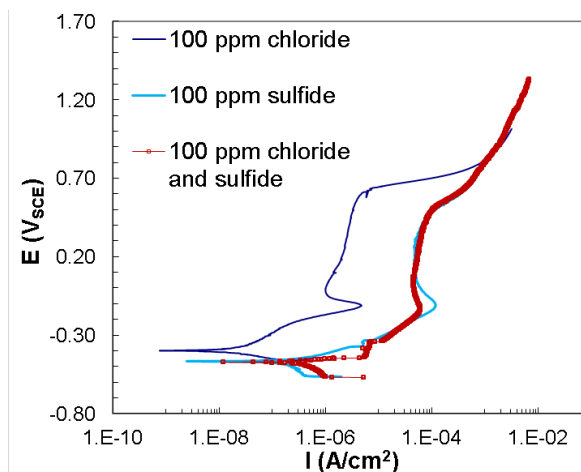
**(d)**

**Figure 2-8. (a) OCP and (b) Potentiodynamic Polarization of Carbon Steel in Ca(OH)$_2$ and Ca(OH)$_2$ With the Addition of 100 ppm Cl$^-$, S$_2$O$_3$$^{2-}$, and S$^{2-}$, Separately at 80 °C [176 °F]; Comparison of (c) OCP and (d) Potentiodynamic Scan of Carbon Steel in Ca(OH)$_2$ With the Addition of 100 ppm Cl$^-$ and S$^{2-}$, Separately and Combined at 80 °C [176 °F]**

| Table 2-5. Corrosion Rates of Carbon Steel Exposed to Ca(OH)$_2$ at 80 $^o$C [176 °F] With Cl$^-$, S$_2$O$_3$$^{2-}$, and S$^{2-}$ Addition | | | | |
|---|---|---|---|---|
| Tests | Ca(OH)$_2$ only | Ca(OH)$_2$ + 100 ppm Cl$^-$ | Ca(OH)$_2$ + 100 ppm S$_2$O$_3$$^{2-}$ | Ca(OH)$_2$ + 100 ppm S$^{2-}$ |
| Corrosion rate, μm/yr | 0.29 | 0.55 | 0.70 | 4.7 |
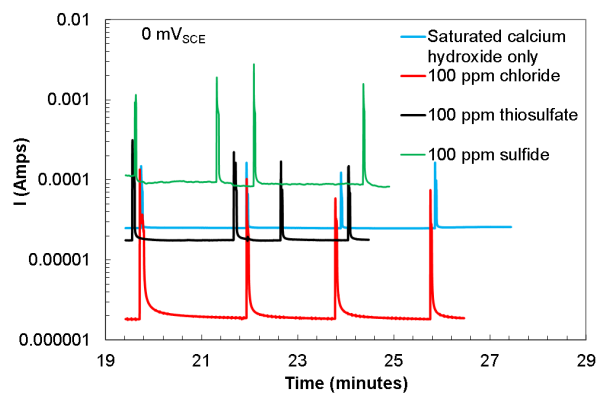
**(a)**
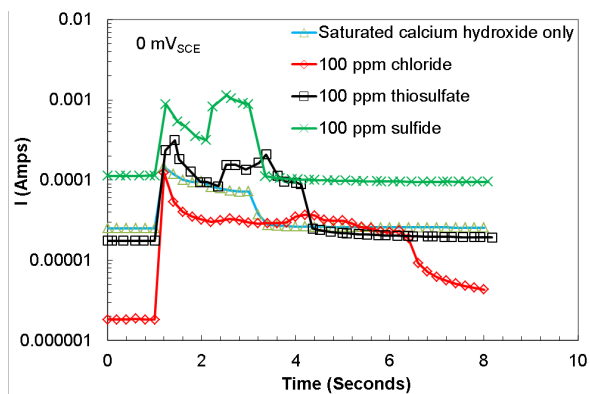
**(b)**
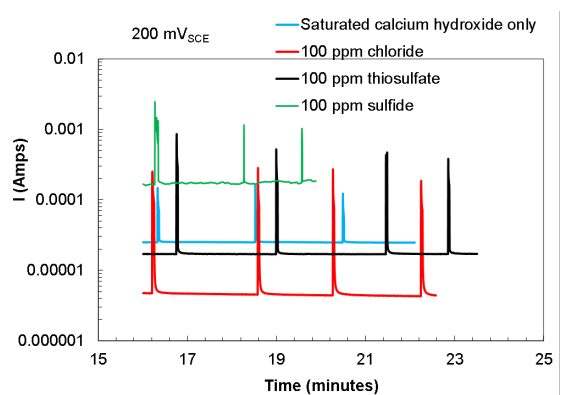
**(c)**
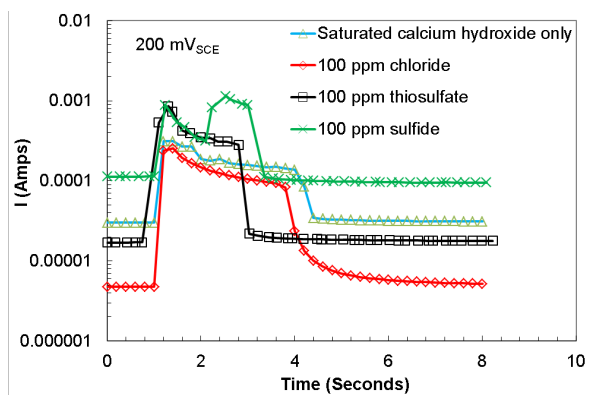
**(d)**
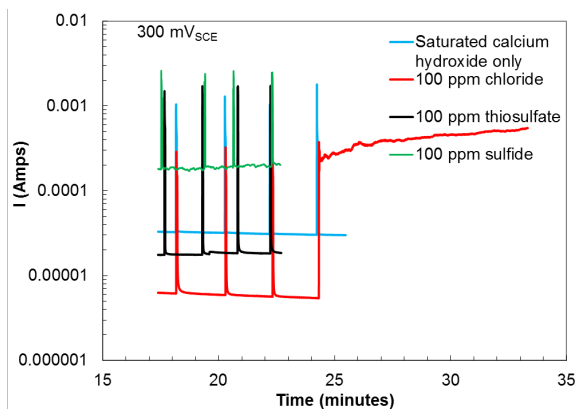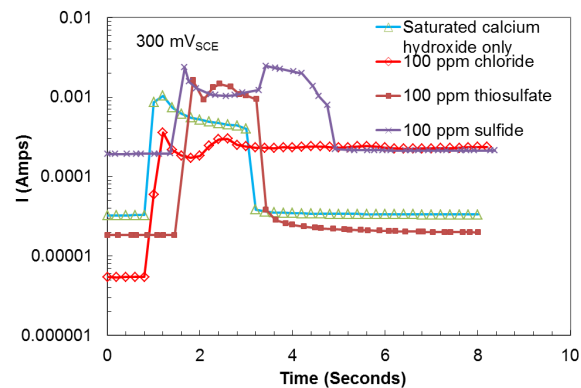
**(e)**                        **(f)**

**Figure 2-9.  Current Versus Time Transient Curves for Carbon Steel When Four Successive Scratches Were Made at Two Locations on the Surface of the Rotating Working Electrodes at Applied Potentials of (a) and (b) 0, (c) and (d) 0.2, and (e) and (f) 0.3 $V_{SCE}$ in Deaerated Ca(OH)$_2$ Solution Without and With the Addition of Cl$^-$, S$_2$O$_3^{2-}$, and S$^{2-}$, Respectively, at 80 °C [176 °F]**

Figures 2-9(b), (d), and (f) are expanded views of the first transient at each polarization potential.  For all tested samples up to 0.5 $V_{SCE}$ with and without addition of $S_2O_3^{2-}$ and $S^{2-}$ to the Ca(OH)$_2$ solution, once a passive film was mechanically disrupted by scratching, the anodic current increased abruptly to the peak current and thereafter decreased as repassivation occurred, typically in 2 to 3 seconds.  Figures 2-9(e) and (f) show that with the addition of Cl$^-$, at the polarization potential of 0.3 $V_{SCE}$, the material completely lost its passivity after scratching.  In the meantime, pitting, as shown in Figure 2-10, was observed on the electrode.
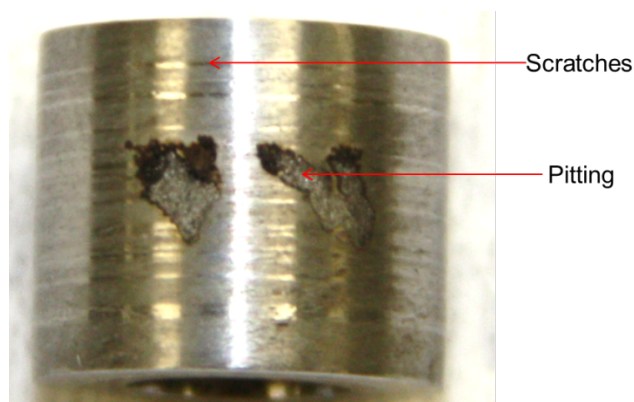


**Figure 2-10.  Carbon Steel Specimen After Scratch Test in Deaerated Ca(OH)$_2$ Solution With the Addition of Cl$^-$ After Polarizing to 0.3 $V_{SCE}$**

2-13

# 3   COPPER CORROSION TESTS IN SIMULATED GRANITIC WATER

## 3.1      Experimental Approaches

### 3.1.1      Material

An oxygen-free high conductivity copper rod composed of alloy 101 (the highest purity grade of copper at 99.99 percent), 6.4 mm [0.25 in] diameter, was used in the electrochemical tests.  The rod was cut into cylindrical electrodes 50 mm [2 in] long.

Oxygen free copper foil with a copper concentration of 99.997 percent, 0.25 mm [0.01 in] thick, was used in the immersion test.

### 3.1.2      Simulated Granitic Water

Groundwaters in granitic rocks tend to become increasingly saline with depth, and they are characterized by reducing conditions.  At a nominal repository depth {e.g., 500 m [1,640 ft]}, the groundwaters commonly are close to thermodynamic equilibrium with secondary mineral phases such as calcite (calcium carbonate) or gypsum (calcium sulfate), and carbonate concentrations are variable but typically low.  A repository constructed in a granitic host rock is likely to use an engineered barrier such as bentonite to reduce the likelihood of advection near the waste containers.  Reactions between the bentonite and the groundwater will initially alter the composition of near-field water contacting the container and, if the container fails, that of the water contacting the spent fuel waste form.  For example, ion exchange reactions between the bentonite and the contacting water are likely to increase the Na concentration and decrease the Ca concentration of the water, and, if gypsum ($CaSO_4 \cdot 2H_2O$) is a trace mineral in the bentonite, its dissolution will tend to increase the concentration of sulfate ions.  These effects are more pronounced in the early stages of saturation of the bentonite.  As more pore volumes of groundwater pass through the bentonite over time in a repository setting, the near-field water chemistry will return to a composition more similar to the surrounding groundwater.  At a nominal repository depth of about 500 m [1,640 ft] the $SO_4^{2-}$ concentrations in Swedish groundwater samples range from near 0 to values approaching 600 mg/L (King, et al., 2010b, Figure 4-6).

For the copper corrosion experimental work, a solution composition was selected to be representative of a deep groundwater chemistry that is likely to be present at nominal repository depth in a massive crystalline bedrock such as granite (McMurry, 2014).  The solution composition is based on reference Canadian Shield groundwater compositions identified by various nuclear waste management research programs (e.g., Gascoyne, 1988; NWMO, 2012), particularly the reference synthetic groundwater WN-1m initially developed for use in sorption experiments from groundwater data collected over depths between 350 and 800 m [1,148 and 2,624 ft] below the surface in crystalline rocks of the Canadian Shield (Gascoyne, 1988).  Its composition is approximately in the mid-range of concentration values for analyzed Canadian Shield groundwaters at depth (e.g., McMurry, 2004, Figures 3 and 4), and it is at or near equilibrium with calcite.  The simulated groundwater composition in this study along with the compositions in Gascoyne (1988) and NWMO (2012) is shown in Table 3-1, and the recipe to prepare 10 L [2.6 gal] of the solution from reagents is shown in Table 3-2.

**Table 3-1. Comparison of Three Reference Groundwaters for Deep Crystalline Rocks**

| Species | Concentration (M) | | |
|---|---|---|---|
| | Reference Simulated Groundwater (This Study) | Synthetic Groundwater WN-1m* | Reference Deep Groundwater CR-10† |
| $Na^+$ | $8.0 \times 10^{-2}$ | $8.0 \times 10^{-2}$ | $8.0 \times 10^{-2}$ |
| $Ca^{+2}$ | $1.0 \times 10^{-2}$ | $5.0 \times 10^{-2}$ | $5.0 \times 10^{-2}$ |
| $Mg^{+2}$ | $3.0 \times 10^{-3}$ | $3.0 \times 10^{-3}$ | $2.5 \times 10^{-3}$ |
| $K^+$ | $4.0 \times 10^{-4}$ | $4.0 \times 10^{-4}$ | $3.8 \times 10^{-4}$ |
| $Cl^-$ | $9.2 \times 10^{-2}$ | $2.0 \times 10^{-1}$ | $2.0 \times 10^{-1}$ |
| $SO_4^{-2}$ | $7.0 \times 10^{-3}$ | $9.0 \times 10^{-3}$ | $1.0 \times 10^{-2}$ |
| $HCO_3^-$ | $8.9 \times 10^{-4}$ | $1.0 \times 10^{-3}$ | $1.1 \times 10^{-3}$ |

*Gascoyne, M. "Reference Groundwater Composition for a Depth of 500 m in the Whiteshell Research Area—Comparison With Synthetic Groundwater WN-1." Report AECL TR-463. Pinawa, Canada: Atomic Energy of Canada Limited. 1988.
†NWMO. "Used Fuel Repository Conceptual Design and Postclosure Safety Assessment in Crystalline Rock." Pre-Project Report NWMO TR-2012-16. Toronto, Canada: Nuclear Waste Management Organization. 2012.

**Table 3-2. Recipe for Preparing 10 L [2.6 gal] Simulated Granitic Groundwater in This Study**

| Reagent | Target amount of reagent {g/10 L [oz/2.6 gal] of solution} |
|---|---|
| NaCl | 38.0 [1.34] |
| KCl | 0.3 [0.01] |
| $Na_2SO_4$ | 10.0 [0.35] |
| $CaCl_2.2H_2O$ | 15.0 [0.53] |
| $MgCl_2.6H_2O$ | 6.0 [0.21] |
| $NaHCO_3$ | 0.75 [0.026] |
| Measured pH | 6.65 |

### 3.1.3 Corrosion Rates and Hydrogen Generation Measurement

Electrochemical impedance spectroscopy (EIS) and linear polarization resistance (LPR) were used to measure corrosion rates of copper exposed to deaerated simulated granitic water at 30, 50, and 80 °C [86, 122, and 176 °F]. The method is the same as that described in Section 2.1.2. Copper cylindrical electrodes were used in the test. The solution was deaerated with ultrahigh purity (UHP) argon gas to maintain an anoxic condition.

Copper foil was immersed in anoxic granitic water in an autoclave for hydrogen generation measurements. The procedure and the autoclave are the same as those described in Section 2.1.3. The tests started at two different internal pressures applied by the inert gas: 1 atm [15 psi] and 3 atm [44 psi]. For the test at 3 atm [44 psi], one autoclave without a specimen was set up for comparison at exactly the same condition.

## 3.2          Results

### 3.2.1          EIS and LPR Measurement for General Corrosion Rates at 30, 50, and 80 °C [86, 122, and 176 °F]

Three tests were conducted with the copper electrodes immersed in the granitic waters at 30, 50, and 80 °C [86, 122, and 176 °F] to measure copper general corrosion rates using EIS and LPR:  (i) started at 30 °C [86 °F], then increased temperature to 50 °C [122 °F], (ii) started at 50 °C [122 °F], then increased temperature to 80 °C [176 °F], (iii) started at 30 °C [86 °F], then increased temperature to 50 and 80 °C [122 and 176 °F].  At the beginning stage at each EIS measurement, open circuit potential (OCP) was measured for 4 days.  Some of the OCP data is shown in Figure 3-1.  At all temperatures, OCP fluctuated in the range of −0.40 to −0.25 $V_{SCE}$.  The test duration at each temperature was about one month.  All the EIS data are shown in Figure 3-2 and they had similar features with one time constant in the measurement frequency range.  The data were fit with a one time-constant Randles circuit.  Corrosion rates were calculated from the polarization resistance using copper density, 8.94 g/cm$^3$ [0.32 lb/in$^3$], and equivalent weight as 31.8 g [0.0701 lb] and are summarized in Table 3-3.  The estimated corrosion rates are several μm/yr [several hundredths mils/yr].  Considering the data uncertainty, there is no clear trend on temperature dependence of the corrosion rates.

After EIS measurement, linear polarization was performed from −10 to 10 mV versus OCP to measure corrosion rate.  Some of the linear polarization curves are shown in Figure 3-3.  Over the small polarization range, the current response is near linear, which allows the data to be fit with a straight line to determine the polarization resistance.  The corrosion rates calculated from the linear polarization curves are also included in Table 3-3.  They were very close to those measured using EIS, which provides further confidence on the measured corrosion rate data using EIS.  One posttest specimen is shown in Figure 3-4 as an example.  The surface was tarnished with black film covered in some area.  There were some white deposits on the specimen above the solution, which was due to the solution evaporation at elevated temperatures.  Examination under microscope shows some localized features, but those featured are too shallow to be characterized as pits.

### 3.2.2          Hydrogen Generation Measurement in Autoclave at 80 °C [176 °F]

#### 3.2.2.1          Test at 1 atm [15 psi] Inert Gas Pressure

Oxygen-free pure copper foil {0.25-mm [9.8 mils] thick} was exposed to anoxic simulated granitic water for 6 months at 1 atm [15 psi].  Gas was sampled at 3 and 6 months for composition analysis.  Hydrogen was detected from both samples.  The hydrogen concentration was 0.180 and 0.202 volume percent, respectively, in the 3 and 6 month samples.  Assuming corrosion of 1 mole of copper released 1 mole of electrons (i.e., generated 0.5 mole of H$_2$; Eq. 1-3),  the corrosion rates were calculated to be 0.076 and 0.084 μm/yr [0.0030 and 0.0032 mils/yr], respectively.

The test was stopped at six months.  The posttest solution in autoclave and specimens are shown in Figure 3-5.  Solution was still clear, but there was black powder at the bottom of the cell.  The copper foil was also tarnished with black film in some area, which is consistent with what was observed in Figure 3-4.  Three posttest copper foils were analyzed for hydrogen content along with one base specimen.  The tested specimens had hydrogen content of 3, 3,
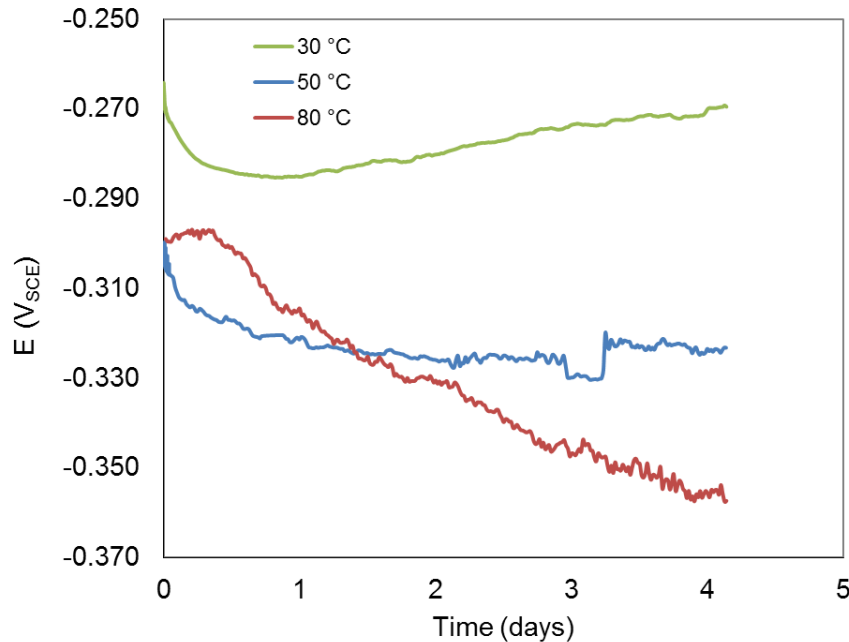
**Figure 3-1.  OCP of Copper Exposed to Anoxic Simulated Granitic Water at 30, 50, and 80 °C [86, 122, and 176 °F] for the First Four Days**

and 5 ppm, but the as-received  untested specimen had hydrogen content of 6 ppm.  This indicates that the hydrogen detected in the tested specimen may not be from the corrosion process.  Further analysis is needed to understand further if there is hydrogen absorbed into the specimen.

### 3.2.2.2　　　Test at 3 atm [44 psi] Inert Gas Pressure

With the heating up of the autoclave, the gauge pressure reading from both autoclaves with and without test specimens increased from the original 2 atm [30 psi] to 3.1 atm [45 psi] at 80 °C [176 °F].  Using the ideal gas law and the 0.9 L [0.24 gal] head space, the pressure increase of the inert gas in the autoclave from 20 to 80 °C [68 to 176 °F] was 0.6 atm [8.8 psi], which is lower than the total pressure increase.  This means that water still evaporated into the head space under the pressurized condition, which led to a pressure increase of 0.5 atm [7.4 psi] associated with water vapor.  Gas was sampled from the head space of each autoclave at 3 months.  The hydrogen concentration was analyzed to be 0.016 and 0.013 volume percent from tests with and without the copper specimen, respectively.  The concentration was slightly above the detection limit of the instrument and one order of magnitude lower than the test in Section 3.2.2.1 conducted at 1 atm [15 psi].  The hydrogen concentration from the autoclave with copper specimen was slightly higher than the one without any specimen, but the difference of 0.003 volume percent is below the detection limit of 0.01 volume percent.  These preliminary results could suggest that hydrogen evolution from copper corrosion is negligible.  The test will continue for another 3 months to confirm the observation.
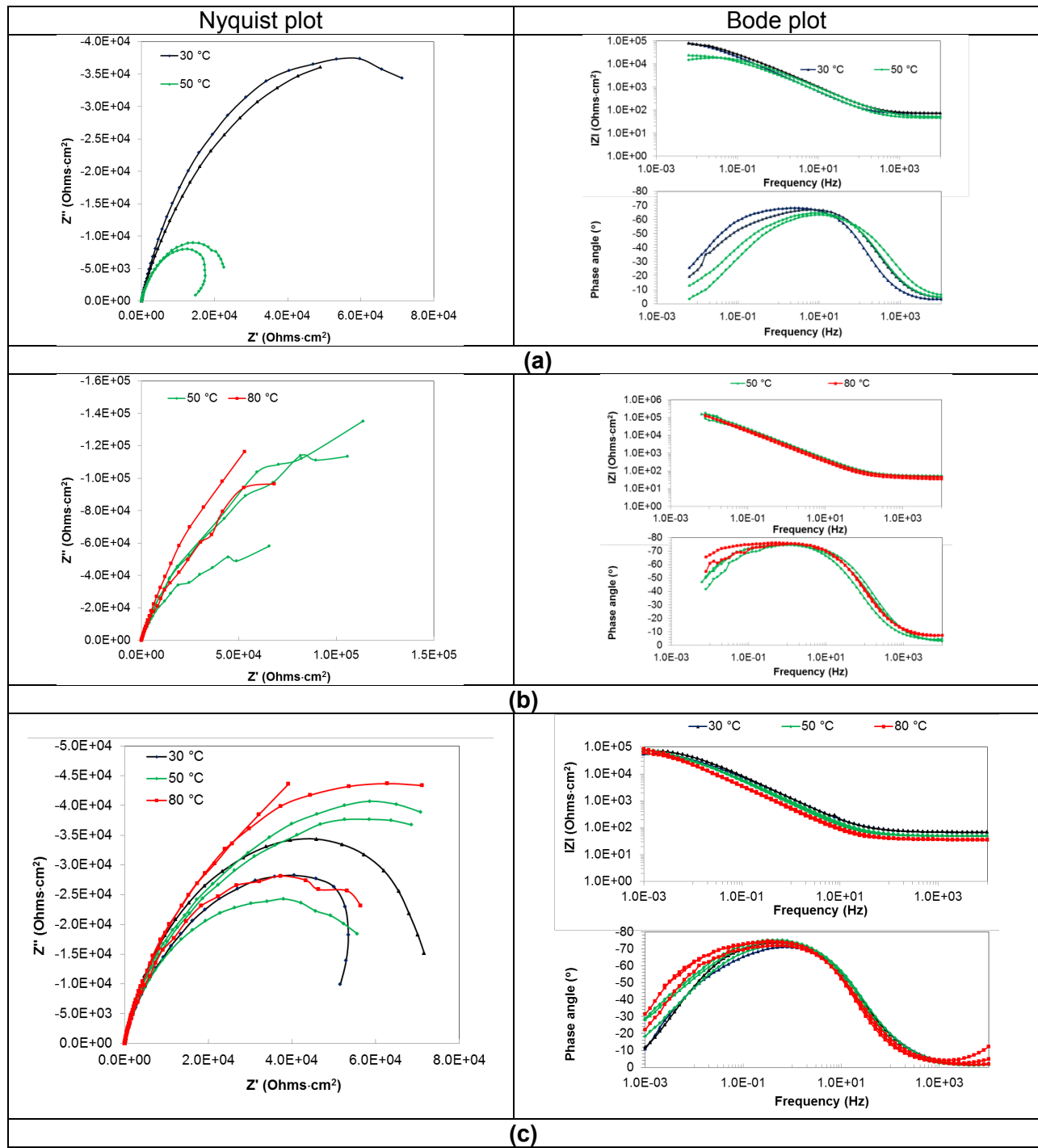
Figure 3-2.  EIS of Copper Exposed to Anoxic Simulated Granitic Water (a) Nyquist, and BodePlots of One Test at 30 and 50 °C [86 and 176 °F], (b) One Test at 50 and 80 °C [122 and 176 °F], (c) One Test at 30, 50, and 80 °C [86, 122, and 176 °F]
In the Nyquist Plot, x and y-axes are the real and imaginary components, respectively, of the impedance. In the Bode Plot, the x-axis is the frequency and the y-axis is the amplitude of the impedance in the top plot and phase angle in the bottom plot.

| Table 3-3. Corrosion Rates of OFHC Copper Exposed to Anoxic Simulated Granitic Water | | | | | | | | | |
|---|---|---|---|---|---|---|---|---|---|
| **Temperature, °C [°F]** | | 30 [86] | | 50 [122] | | | 80 [176] | | |
| **Corrosion rate, µm/yr** | EIS, Test a | 3.2 | 3.6 | 16* | | 13* | Not measured | | |
| | EIS, Test b | Not measured | | 0.83 | 0.95 | 2.4 | 1.0 | | 0.48 |
| | Test c  EIS | 4.6 | 3.7 | 5.0 | 3.5 | 3.4 | 3.0 | 3.0 | 4.4 |
| | LPR | 4.9 | 3.5 | 5.3 | 5.1 | 4.9 | 6.7 | | |
| **Average corrosion rate, µm/yr** | | **3.9 ± 0.7** | | **3.5 ± 1.8** | | | **3.1 ± 2.3** | | |
| *Treated as outliers | | | | | | | | | |



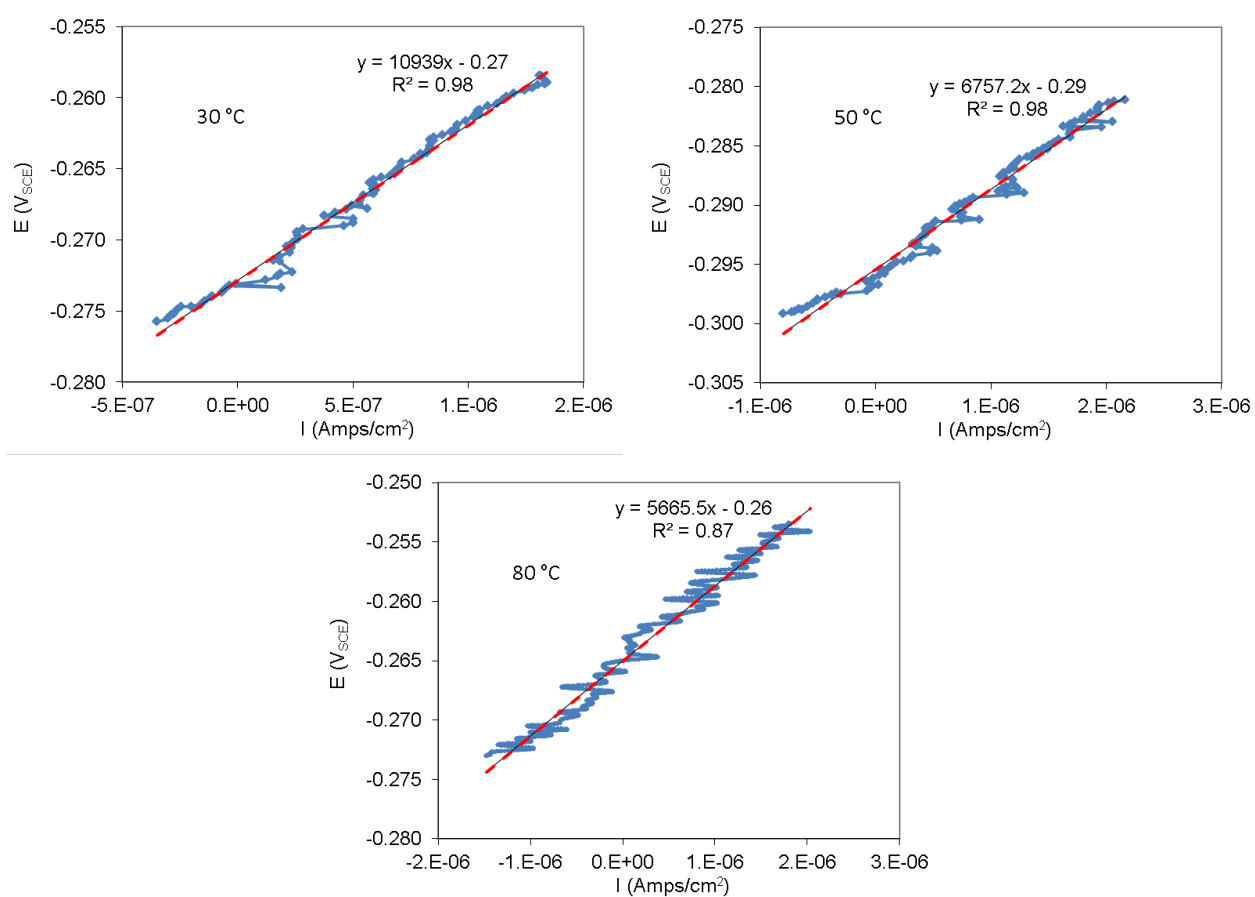**Figure 3-3. Linear Polarization Curves of Copper Exposed to Anoxic Simulated Granitic Water at 30, 50, and 80 °C [86, 122, and 176 °F]**

White deposits from solution evaporation
Section above solution
Solution surface
Section exposed in solution
100 µm
100 µm
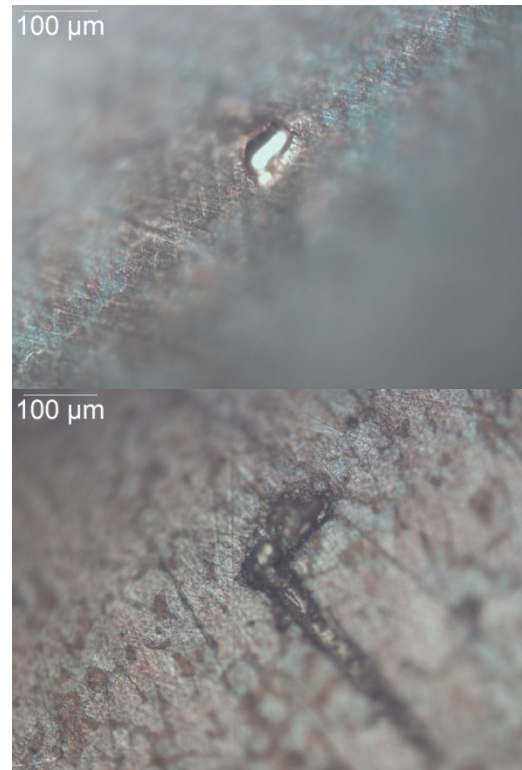
**Figure 3-4.  Example of Posttest Copper Electrodes After Exposing to Anoxic Simulated Granitic Water**

(a)



(b)

**Figure 3-5. Posttest Solution and Copper Foils After Exposure to Anoxic Simulated Granitic Water at 80 °C [176 °F] for 6 Months**

# 4 CONCLUSIONS

This study investigated carbon steel corrosion in anoxic alkaline water and copper corrosion in anoxic simulated granitic water. General corrosion rates, hydrogen generation, and passivity were studied using electrochemical methods. Specific conclusions follow.
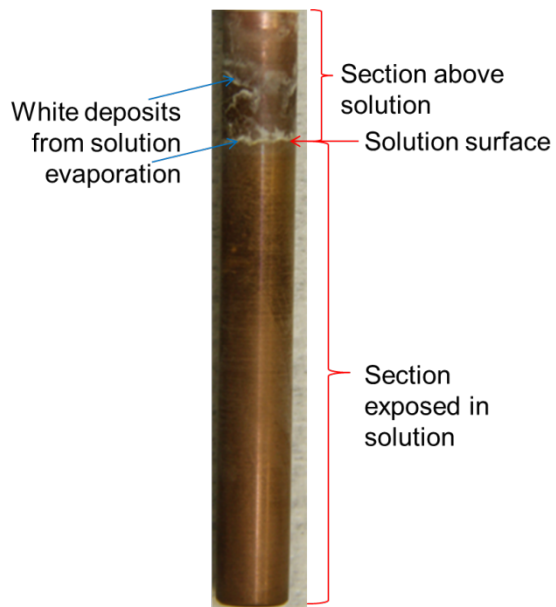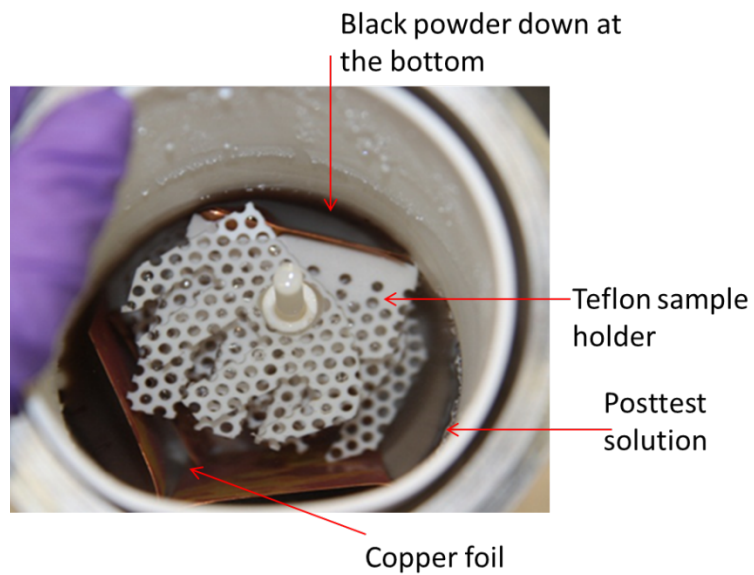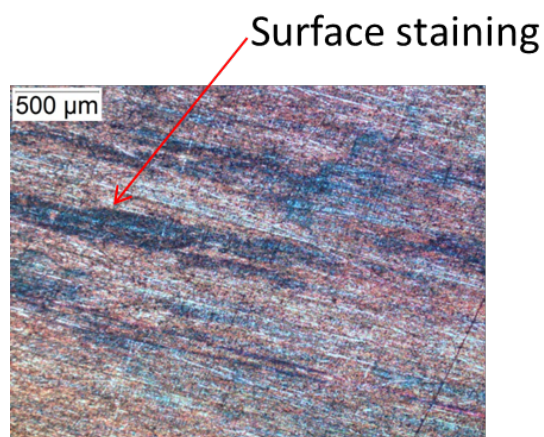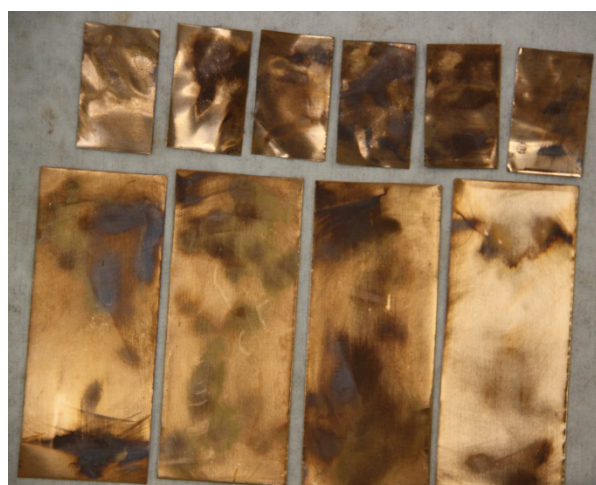
**Carbon Steel**

- Estimated corrosion rates derived from the experimental data ranged from 0.1–3 µm/yr [0.004–0.1 mils/yr] for carbon steel exposed to anoxic alkaline water at 30, 50, and 80 °C [86, 122, and 176 °F]. This is consistent with the range of carbon steel general corrosion rate {0.1–10 µm/yr [0.0039–0.39 mils/yr]} in an anoxic environment used in the U.S. Nuclear Regulatory Commission (NRC) and Center for Nuclear Waste Regulatory Analyses (CNWRA®) SOAR model. The majority of the corrosion rates measured by weight loss and electrochemical methods are within a narrow range.

- Corrosion rates were observed to not depend on temperature at 30, 50, and 80 °C [86, 122, and 176 °F].

- In addition to general corrosion, localized corrosion was observed as represented by a small number of pits.

- Tens to hundreds of ppm of hydrogen was generated from the corrosion process over 3 months at 80 °C [176 °F]. It is estimated that some hydrogen was absorbed into the carbon steel specimen. The absorbed hydrogen content was 3–5 ppm.

- Chloride, thiosulfate, and sulfide increased carbon steel passive dissolution in $Ca(OH)_2$ solution. Chloride increased the dissolution rate the least and sulfide increased it the most. Thiosulfate was intermediate between these two.

- Once a passive film was mechanically disrupted by scratching, carbon steel repassivated in 2 to 3 seconds, both without and with the addition of 100 ppm sulfide and thiosulfate to $Ca(OH)_2$ solution up to 0.5 $V_{SCE}$. However, the material completely lost its passivity after scratching with the addition of 100 ppm chloride at the polarization potential of 0.3 $V_{SCE}$. Carbon steel is more susceptible to pitting in chloride-containing alkaline water.

**Copper**

- Most of the corrosion rates of copper measured by electrochemical methods in anoxic simulated granitic waters (less than 10 ppb) ranged from 1–5 µm/yr [0.039–0.2 mils/yr]. At this $O_2$ level the rates are higher than the general corrosion rate ranges of $4 \times 10^{-3}$ to $2 \times 10^{-2}$ µm/yr [$2 \times 10^{-4}$ to $8 \times 10^{-4}$ mils/yr] used in the NRC and CNWRA SOAR model for reducing environments. These significantly higher copper corrosion rates are at odds with some statements in the literature that argue copper would experience little to no corrosion in a reducing environment, but they do agree with other literature statements that copper corrosion rates could be higher under this environment. The differences among reported corrosion rates could be related to factors such as differing methodologies or experimental solutions. More in-depth analyses are warranted to further understand the differences.

- It was also observed that the copper surface was tarnished after the test.

- Hydrogen from copper immersion in the same anoxic simulated granitic waters was detected from the vapor phase, but not in the metal.  The detected hydrogen could be due to corrosion from the test cell.  Further tests are warranted to confirm the observation.

# 5   REFERENCES

ASTM International.  ASTM A516/A516M–10, "Standard Specification for Pressure Vessel Plates, Carbon Steel, for Moderate- and Lower-Temperature Service." West Conshohocken, Pennsylvania:  ASTM International.  2010.

ASTM International.  ASTM G102–89, "Standard Practice for Calculation of Corrosion Rates and Related Information from Electrochemical Measurements." West Conshohocken, Pennsylvania:  ASTM International.  2004.

Gascoyne, M.  "Reference Groundwater Composition for a Depth of 500 m in the Whiteshell Research Area—Comparison with Synthetic Groundwater WN-1."  Report AECL TR-463. Pinawa, Canada:  Atomic Energy of Canada Limited.  1988.

Hardy, R.  "ITS-90 Formulations for Vapor Pressure, Frost Point Temperature, Dew Point Temperature, and Enhancement Factors in the Range−100 to 100 °C."  The Proceedings of the Third International Symposium on Humidity & Moisture.  London, England:  Teddington.  1998.

He, X., O. Pensado, T. Ahn, P. Shukla.  "Model Abstraction of Stainless Steel Waste Package Degradation."  Proceedings of 2011 International Radioactive Waste Management Conference (IHLRWMC).  Albuquerque, New Mexico:  Vol. 2. pp.  679–686.  2011.

Hultquist, G., P. Szakalos, M.J. Graham, A.B. Belonoshko, G.I. Sproule, L. Grasjo, B. Danilov, T. AAstrup, G. Wilmark, G.-K. Chuah, J.-C. Eriksson, and A. Rosengren.  "Water Corrodes Copper."  *Catalysis Letters*.  Vol. 132.  pp. 311–316.  2009.

Jung, H., T. Ahn, and X. He.  "Representation of Copper and Carbon Steel Waste Package Degradation in a Generic Performance Assessment Model."  Proceedings of 2011 International Radioactive Waste Management Conference (IHLRWMC), Albuquerque, New Mexico. Vol. 2. pp. 672–678. 2011.

King, F.  "Container Materials for the Storage and Disposal of Nuclear Waste."  *Corrosion*. Vol. 69.  pp. 986–1,011.  2013.

King, F.  "Canister Materials for the Disposal of Nuclear Waste."  *Comprehensive Nuclear Materials*.  Oxford, United Kingdom:  Elsevier.  Ch. 131.  2010a.

King, F.  "An Update of the State-of-the-Art Report on the Corrosion of Copper Under Expected Condition in a Deep Geologic Repository."  Stockholm, Sweden:  Swedish Nuclear Fuel and Waste Management Co.  2010b.

King, F.  "Overview of a Carbon Steel Container Corrosion Model for a Deep Geological Repository in Sedimentary Rock."  NWMO TR-2007-01.  Nuclear Waste Management Organization.  2007.

King, F. and S. Watson.  "Review of the Corrosion Performance of Selected Metals as Canister Materials for UK Spent Fuel and/or HLW."  QRA-1384J-1.  United Kingdom:  Nuclear Decommissioning Authority.  2010.

King, F., C. Lilja, K. Pedersen, P. Pitkänen, and M. Vähänen. "An Update of the State-of-the-Art Report on the Corrosion of Copper Under Expected Conditions in a Deep Geologic Repository." SKB Technical Report TR-10-67. Stockholm, Sweden: Swedish Nuclear Fuel and Waste Management Company. 2010.

Kursten, B., F. Druyts, D.D. Macdonald, N.R. Smart, R. Gens, L. Wang, E. Weetjens, and J. Govaerts. "Review of Passive Corrosion Studies of Carbon Steel in Concrete in the Context of Disposal of Passive Corrosion Studies of Carbon Steel in Concrete in the Context of Disposal of HLW and Spent Fuel in Belgium." Proceedings of the ASME 2013 15th International Conference on Environmental Remediation and Radioactive Waste Management. ICEM2013. September 8–12, 2013. Brussels, Belgium: ICEM2013-96275. 2013.

Kursten, B., F. Druyts, D.D. Macdonald, N.R. Smart, R. Gens, L. Wang, E. Weetjens, and J. Govaerts. "Review of Corrosion Studies of Metallic Barrier in Geological Disposal Conditions with Respect to Belgian Supercontainer Concept." *Corrosion Engineering, Science and Technology*. Vol. 46. pp. 91–97. 2011.

Lu, P., A. Almarzooqi, B. Kursten, and D. Macdonald. "Corrosion of Carbon Steel in Simulated Concrete Pore Water under Anoxic Conditions." 5th International Workshop on Long Term Prediction of Corrosion Damage in Nuclear Waste Systems. Asahikawa. Japan. 2013.

Macdonald, D.D., S. Sharifi, A. Almarzooqi, G.R. Engelhardt, and B. Kursten. "Electrochemical Impedance Modeling of the Passivity of Carbon Steel in Simulated Concrete Pore Water." *ECS Transactions*. Vol. 50. pp. 41–56. 2013.

Markley, C., E.L. Tipton, J. Winterle, O. Pensado, J.-P. Gwo. "β-SOAR: A Flexible Tool for Analyzing Disposal of Nuclear Waste." Proceedings of 2011 International Radioactive Waste Management Conference (IHLRWMC), Albuquerque, New Mexico. Vol. 2. pp. 753–758. 2011.

McMurry, J. "Synthesis of Groundwater Test Solutions." Scientific Notebook 1228E. San Antonio, Texas: Center for Nuclear Waste Regulatory Analyses. pp. 1–39. 2014.

McMurry, J. "Reference Water Compositions for a Deep Geologic Repository in the Canadian Shield." Report OPG 06819-REP-01200-10135-R01. Toronto, Canada: Ontario Power Generation. 2004.

Newman, R.C., S. Wang, L. Johnson, and N. Diomidis. "Carbon Steel Corrosion and Hydrogen Gas Generation in Cementitious Grout under Anoxic Conditions." 5th International Workshop on Long Term Prediction of Corrosion Damage in Nuclear Waste Systems. Asahikawa, Japan. 2013.

NWMO. "Used Fuel Repository Conceptual Design and Postclosure Safety Assessment in Crystalline Rock." Pre-Project Report NWMO TR-2012-16. Toronto, Canada: Nuclear Waste Management Organization. 2012.

Pourbaix, M. *Atlas of Electrochemical Equilibria in Aqueous Solutions*. 2nd ed. Houston, Texas: NACE. 1974.

Roseborg, B. and L. Werme. "The Swedish Nuclear Waste Program and the Long-Term Corrosion Behavior of Copper." *Journal of Nuclear Materials*. Vol. 379. pp.124–153. 2008.

Scully, J.R. and T.W. Hicks. "Initial Review Phase for SKB's Safety Assessment SR-Site: Corrosion of Copper." Swedish Radiation Safety Authority Technical Note 2012:21. 2012.

Smart, N.R., A.P. Rance, P.A.H. Fennell, and B. Kursten. "The Anaerobic Corrosion of Carbon Steel in Alkaline Media—Phase 2 Results." *EPJ Web of Conferences*. Vol. 56. 06003. 2013.

Urquidi-Macdonald, M., A. Almarzooqi, B. Kursten, and D.D. Macdonald. "On the Stability of the Passive Film on Carbon Steel as Indicated by Electrochemical Impedance Spectroscopy." *ECS Transactions*. Vol. 50. pp. 283–299. 2013.